Tetrazine derived mononuclear $Ru^{II}(acac)_2(L)$ (**1**), $[Ru^{II}(bpy)_2(L)](ClO_4)_2$ (**2**) and $[Ru^{II}(bpy)(L)_2](ClO_4)_2$ (**3**) (L = 3-amino-6-(3,5-dimethylpyrazol-1-yl)-1,2,4,5-tetrazine, acac = acetylacetonate, bpy = 2,2′-bipyridine): syntheses, structures, spectra and redox properties

Animesh Nayak [a], Srikanta Patra [a], Biprajit Sarkar [b], Sandeep Ghumaan [a], Vedavati G. Puranik [c], Wolfgang Kaim [b,*], Goutam Kumar Lahiri [a,*]

[a] *Department of Chemistry, Indian Institute of Technology – Bombay, Powai, Mumbai 400 076, India*
[b] *Institut für Anorganische Chemie, Universität Stuttgart, Pfaffenwaldring 55, D-70550 Stuttgart, Germany*
[c] *Center for Materials Characterization, National Chemical Laboratory, Pune, Maharashtra 411 008, India*

Abstract

Mononuclear ruthenium complexes of tetrazine derived L, $Ru^{II}(acac)_2(L)$ (**1**), $[Ru^{II}(bpy)_2(L)](ClO_4)_2$ (**2**) and $[Ru^{II}(bpy)(L)_2](ClO_4)_2$ (**3**) (L = 3-amino-6-(3,5-dimethylpyrazol-1-yl)-1,2,4,5-tetrazine, acac = acetylacetonate and bpy = 2,2′-bipyridine) were prepared. The free L exists as a dimeric entity in the solid state via hydrogen bonding interactions involving L and water molecules present in the crystal lattice. **1** exhibits unusually strong bonds from Ru^{II} to coordinating pyrazolyl-N (2.040(2) Å) and especially to tetrazine-N (1.913(2) Å). The Ru^{III}/Ru^{II} couples of **1**–**3** appeared at 0.28, 1.34 and 1.50 V versus SCE, respectively. The tetrazine and bpy-based reductions were observed at −1.33 (**1**); −0.55 and −1.55/−1.75/−1.98 (**2**); −0.47/−0.78 and −1.80/−2.02 V (**3**), respectively. **1**, **2** and **3** displayed two MLCT bands each, corresponding to $d\pi(Ru^{II}) \rightarrow \pi^*$ (L, tetrazine) and $d\pi(Ru^{II}) \rightarrow \pi^*$ (acac or bpy or L) transitions. $\mathbf{1}^+$ and $\mathbf{2}^+$ showed rhombic EPR spectra at 110 and 4 K, respectively and $\mathbf{1}^-$, $\mathbf{2}^-$ and $\mathbf{3}^-$ exhibited multiple line EPR spectra at 300 K. **1**–**3** exhibited moderately strong emission spectra in EtOH–MeOH glass at 77 K.

Keywords: Ruthenium–tetrazine; Synthesis; Structure; Electrochemistry; Redox; Spectra

1. Introduction

Among the well established polynucleating ligands in coordination chemistry are the 3,6-disubstituted 1,2,4,5-tetrazines [1]. During the last decade these ligands have become more and more popular because of their special electronic and structural properties. The electronic properties are related to the strong π-accepting nature of the tetrazine moiety due to the low-lying π* MO, while the structural features are essentially based on the efficient metal–metal bridging capacity.

The ability of tetrazine ligand systems to function as efficient electronic spacers between individual metal centers is reflected in a series of diruthenium complexes

encompassing a variety of 3,6-disubstituted tetrazine derivatives [2]. Their structural, spectroelectrochemical, EPR, magnetic and luminescence aspects have been thoroughly investigated. However, only a limited number of *mononuclear* ruthenium–tetrazine derivatives are known so far, e.g., $[(trpy)Ru(bphtz)](PF_6)_2$ [3a], $[(CO)(PPh_3)_2(H)Ru(bptz)]PF_6$ [3b], $[(NH_3)_4Ru(bptz)](PF_6)_2$ [3c,d], $[(bpy)_2Ru(bptz)](PF_6)_2$ [3d], $[\{(CH_3)_2SO\}_2(Cl)_2Ru(bptz)]\cdot mH_2O$ [3e] and $[(bpz)_2Ru(bptz)](PF_6)_2$ [3d,f] [bptz = 3,6-bis(2-pyridyl)-1,2,4,5-tetrazine; bphtz = 3,6-bis(1,10-phenanthroline)-1,2,4,5-tetrazine; trpy = 2,2′:6′,2″-terpyridine; bpz = 2,2′-bipyrazine].

This situation has prompted the present program of exploring the metallation aspects of 3-amino-6-(3,5-dimethylpyrazol-1-yl)-1,2,4,5-tetrazine (L), comprising of a five-membered pyrazolyl ring on one side of the tetrazine and an $-NH_2$ group on the other side. Although L has been synthesized previously [4], its structural and metallation aspects have not been investigated so far. As part of our systematic approach, we report in this paper the synthesis of three ruthenium complexes, viz., $[Ru^{II}(acac)_2(L)]$ (**1**), $[Ru^{II}(bpy)_2(L)](ClO_4)_2$ (**2**) and $[Ru^{II}(bpy)(L)_2](ClO_4)_2$ (**3**), incorporating ancillary ligands such as σ-donating acetylacetonato ($acac^-$) or π-acidic 2,2′-bipyridine (bpy). The crystal structures of L, **1** and **2**, their spectro-electrochemical and luminescence behavior, and the EPR characteristics of the in situ generated Ru^{III} derivatives ($\mathbf{1}^+$, $\mathbf{2}^+$, $\mathbf{3}^+$) and the reduced radical species ($\mathbf{1}^-$, $\mathbf{2}^-$, $\mathbf{3}^-$) are being reported here.

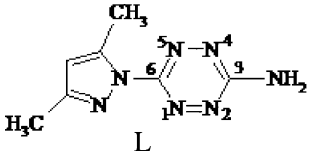

L

2. Experimental

2.1. Materials

The starting complexes $Ru(acac)_2(CH_3CN)_2$ [5], $Ru(bpy)_2Cl_2\cdot 2H_2O$ [6] and $Ru(bpy)Cl_3$ [7] were prepared according to the reported procedures. The ligand 3-amino-6-(3,5-dimethylpyrazol-1-yl)-1,2,4,5-tetrazine was prepared via a modification of the procedure developed by Glidewell et al. [4]. Other chemicals and solvents were reagent grade and were used as received. For spectroscopic and electrochemical studies HPLC grade solvents were used. Commercial tetraethylammonium bromide was converted into pure tetraethylammonium perchlorate following a published procedure [8].

2.2. Physical measurements

UV–Vis spectra were recorded with a JASCO V-570 spectrophotometer. FT-IR spectra were taken on a Nicolet spectrophotometer with samples prepared as KBr pellets. Solution electrical conductivity was checked using a Systronic 305 conductivity bridge. Magnetic susceptibility was checked with a CAHN electrobalance 7550 model sample magnetometer. ^1H NMR spectra were obtained with a 300 MHz Varian FT spectrometer. The elemental analyses were carried out with a Perkin–Elmer 240C elemental analyzer. The EPR measurements were made in a two-electrode capillary tube [9] with an X-band Bruker system ESP300, equipped with a Bruker ER035M gaussmeter and a HP 5350B microwave detector. Cyclic voltammetric, differential pulse voltammetric and coulometric measurements were carried out using a PAR model 273A electrochemistry system. Platinum wire working and auxiliary electrodes and an aqueous saturated calomel reference electrode (SCE) were used in a three-electrode configuration. The supporting electrolyte was $[NEt_4]ClO_4$ and the solute concentration was $\sim 10^{-3}$ M. The half-wave potential E^0_{298} was set equal to $0.5(E_{pa} + E_{pc})$, where E_{pa} and E_{pc} are anodic and cathodic cyclic voltammetric peak potentials, respectively. A platinum wire-gauze working electrode was used in coulometric experiments. All experiments were carried out under a dinitrogen atmosphere and were uncorrected for junction potentials. Electrospray mass spectra were recorded on a Micromass Q-ToF mass spectrometer. Steady state emission experiments were made using a Perkin–Elmer LS 55 luminescence spectrometer fitted with a cryostat. The quantum yields of the complexes were with reference to the reported quantum yield of $[Ru(bpy)_3](PF_6)_2$ in EtOH–MeOH (4:1) solution ($\Phi_{em,77\ K} = 0.35$) [10].

2.3. Preparation of L and complexes *1*, *2* and *3*

2.3.1. Preparation of L, [3-amino-6-(3,5-dimethyl pyrazol-1-yl)-1,2,4,5-tetrazine]

The ligand L was synthesized via a modification (Scheme 1) of the method reported by Glidewell et al. [4]. The ligand bpytz (300 mg, 1.11 mmol) in 20 ml toluene was treated dropwise with 0.3 ml of ammonia at 298 K. The stirring was continued for 2.5 h. The orange solid thus obtained was filtered and washed with toluene and then dried in vacuum. Yield: 170 mg (80%). ^1H NMR in $(CD_3)_2SO$ δ (ppm), 2.20 (s, CH_3), 2.37 (s, CH_3), 6.17 (s, CH), 8.2 (s, NH_2).

2.3.2. $[Ru^{II}(acac)_2(L)]$ (*1*)

The starting complex $Ru(acac)_2(CH_3CN)_2$ (100 mg, 0.26 mmol) and the ligand L (50 mg, 0.26 mmol) were dissolved in 20 ml of ethanol, and the mixture was heated under reflux for 8 h in air. The initially orange

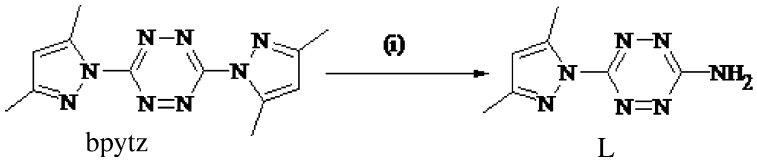

Scheme 1. NH_3, toluene.

solution gradually changed to blue. The solvent was evaporated to dryness under reduced pressure and the solid mass thus obtained was purified by using a silica gel column. Initially, a red compound corresponding to $Ru(acac)_3$ was eluted by CH_2Cl_2–CH_3CN (5:1). With CH_2Cl_2–CH_3CN (1:1), a blue compound corresponding to **1** was separated later. Evaporation of solvent under reduced pressure yielded complex **1**. Yield: **1** (52 mg, 40%). *Anal.* Calc. for complex **1**: C, 41.54; H, 4.69; N, 19.96. Found: C, 41.14; H, 4.33; N, 19.81%. IR, ν/cm^{-1}: 3432 and 3293 ($-NH_2$).

2.3.3. $[Ru^{II}(bpy)_2(L)](ClO_4)_2$ (2)

A mixture of $[Ru(bpy)_2Cl_2]\cdot 2H_2O$ (100 mg, 0.19 mmol) and $AgClO_4$ (100 mg, 0.5 mmol) in 20 ml ethanol was heated with constant stirring for 2 h. The removal of the AgCl precipitate using a sintered-glass funnel resulted in a clear solution containing $[Ru(bpy)_2(EtOH)_2](ClO_4)_2$. To this solution the ligand (L) (39 mg, 0.21 mmol) was added and the mixture was heated under reflux for 5 h in air. The initially red solution gradually changed to purple. The volume of the solution was reduced to about 5 ml under reduced pressure and kept overnight at 268 K. A dark precipitate thus obtained was filtered and washed with cold water followed by cold ethanol. The dried product was then purified by using an alumina column. The purple compound **2** was eluted by CH_3CN. Evaporation of solvent under reduced pressure yielded complex **2**. Yield: **2** (100 mg, 60%). *Anal.* Calc. for complex **2**: C, 40.35; H, 3.14; N, 19.18. Found: C, 40.68; H, 2.87; N, 19.55%. Λ_M/Ω^{-1} ($cm^2\,mol^{-1}$) in MeCN at 298 K: 210. IR, ν/cm^{-1}: 3436/3322 ($-NH_2$) and 1088/618 ClO_4^-.

2.3.4. $[Ru^{II}(bpy)(L)_2](ClO_4)_2$ (3)

A mixture of $Ru(bpy)Cl_3$ (100 mg, 0.27 mmol) and the ligand (L) (130 mg, 0.68 mmol) in ethanol was heated to reflux in air for 12 h. The initially brownish solution gradually changed to purple. The solvent of the reaction mixture was then evaporated to dryness under reduced pressure and the solid mass thus obtained was purified by using a silica gel column. A purple compound containing $[Ru(bpy)(L)_2](ClO_4)_2$ was eluted with 4:1 acetonitrile–methanol mixture. The solvent was evaporated to dryness under reduced pressure, the solid mass was dissolved in the minimum volume of acetonitrile, and an aqueous solution of excess $NaClO_4$ was added to the solution. The dark complex **3** was filtered and washed thoroughly with ice-cold water. Yield: (80 mg, 43%). *Anal.* Calc. for complex **3**: C, 34.38; H, 3.13; N, 26.73. Found: C, 34.53; H, 3.59; N, 22.27%. (Repeated measurements showed the lower 'N' value, typical of compounds containing tetrazine). Λ_M/Ω^{-1} ($cm^2\,mol^{-1}$) in MeOH at 298 K: 220. IR, ν/cm^{-1}: 3429/3318 ($-NH_2$) and 1097/629 (ClO_4^-).

2.4. X-ray structure determination

Single crystals for L and **1** were grown by slow diffusion of a dichloromethane solution into *n*-hexane, followed by slow evaporation. For **2**, an acetonitrile solution was allowed to diffuse slowly into benzene, followed by slow evaporation. X-ray data of L and **1/2** were collected on a PC-controlled Enraf–Nonius CAD-4 (MACH-3) and on a Bruker SMART APEX CCD single crystal X-ray diffractometer, respectively. The structures were solved and refined by full-matrix least-squares techniques on F^2 using the SHELX-97 (SHELXTL program package) [11]. SADABS correction was applied for **1** and **2**. All the data were corrected for Lorentz, polarization and absorption effects.

3. Results and discussion

3.1. Synthesis and characterization of L, 1, 2 and 3

The formation of L was authenticated by its single crystal X-ray structure (Fig. 1). The asymmetric unit contains two molecules of L and two water molecules, all crystallographically independent. The crystal structure of L reveals that it crystallizes as a dimer which is held together via hydrogen bonding interactions involving L and H_2O molecules present in the lattice. Important crystallographic data are summarized in Table 1. Selected bond distances and bond angles for one molecule (molecule A) are listed in Table 2, as bond distances and angles of molecule B are close to those for molecule A. The bond parameters are comparable with standard values [2b,12].

In order to synthesize ruthenium complexes of L incorporating ancillary ligands of a differing electronic nature we chose metal precursors encompassing σ-donating acetylacetonate $\{Ru(acac)_2\}$ and π-acidic bipyridine $\{Ru(bpy)_2^{2+}\}$ and $\{Ru(bpy)^{3+}\}$ cores. The reaction of L and $Ru^{II}(acac)_2(CH_3CN)_2$ in ethanol, followed by chromatographic purification using a silica gel

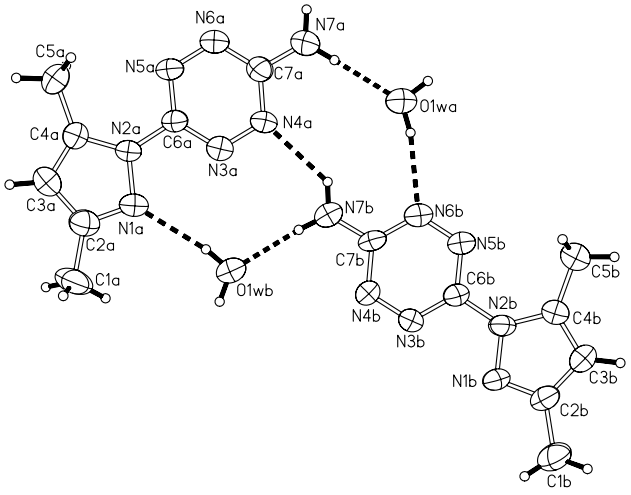

Fig. 1. Asymmetric unit of L.

column, yielded the blue diamagnetic complex $[Ru^{II}(acac)_2L]$ (**1**) (Scheme 2).

Similarly, the reactions of L with $[Ru^{II}(bpy)_2(EtOH)_2]^{2+}$ and $Ru^{III}(bpy)Cl_3$ in ethanol under atmospheric conditions, followed by chromatographic purification, afforded the 1:2 conducting diamagnetic complexes $[Ru^{II}(bpy)_2L](ClO_4)_2$ (**2**) and $[Ru^{II}(bpy)(L)_2](ClO_4)_2$ (**3**), respectively (Scheme 2). During the course of the reaction the +3 oxidation state of the metal ion in the precursor complex $Ru^{III}(bpy)Cl_3$ was reduced to the Ru^{II} state in **3**, even under atmospheric conditions. The replacement of electron rich Cl^- ligands by the strongly π-acidic L stabilizes the metal ion in the +2 state, reflected also by the high redox potential of **3** (see later).

All our attempts to bind a second metal complex fragment via the other tetrazine nitrogen donor center (N4) and the pendant NH_2 group or its anionic form failed altogether. On all occasions the monomeric species **1**–**3** were obtained.

The neutral compound **1** is soluble in non-polar solvents such as CH_2Cl_2 or $CHCl_3$ whereas **2** and **3** are soluble in polar solvents such as CH_3CN and CH_3OH. The NH_2 vibrations of coordinated L and the ClO_4^- vibrations appear near 3300 and 1100/630 cm^{-1}, respectively (see Section 2). The electrospray mass spectra of **1** in CH_2Cl_2 and of **2** and **3** in CH_3CN show maximum molecular ion peaks (*m*/*z*) at 492.23, 704.24 and 739.12, respectively (Fig. S1), corresponding to $[\mathbf{1}]^+$ (calculated molecular mass: 491.08), $\{[\mathbf{2}]\text{-}ClO_4\}^+$ (calculated molecular mass: 704.09) and $\{[\mathbf{3}]\text{-}ClO_4\}^+$ (calculated molecular mass: 739.10).

3.2. Crystal structures of the complexes

The formation of **1** and **2** was confirmed by single crystal X-ray structures (Figs. 2 and 3). Important crystallographic parameters are given in Table 1, selected bond distances and bond angles are listed in Table 2. The single crystal of **1** contains 0.5 equivalents of H_2O of crystallization. The RuO_4N_2 coordination sphere is slightly distorted octahedral as can be seen from the angles at the metal (Table 2). Although the bite angles involving the acac ligands in **1** are close to the ideal value at 90.95(8)° and 93.19(8)°, the bite angle involving L is only 80.11(9)°, reflecting the smaller chelate ring size. The average *trans* angle is 177.41(11)°. The Ru^{II}–O distances vary between 2.0312(19) and 2.048(2) Å. These are comparable to reported Ru^{II}–O(acac) distances [2d]. The Ru^{II}–N(1)(pyrazolyl) and Ru^{II}–N(4)(tetrazine) distances in **1** are 2.040(2) and 1.913(2) Å, respectively, showing the expected stronger bonding to the better π-accepting tetrazine ring. The Ru^{II}–N(pyrazolyl) distance in **1** is distinctly shorter than that found in

Table 1
Crystallographic data for $L \cdot H_2O$, $[Ru^{II}(acac)_2L] \cdot 0.5H_2O$ (**1**) and $[Ru^{II}(bpy)_2L](ClO_4)_2$ (**2**)

	L	**1**	**2**
Formula	$2(C_7H_9N_7) \cdot 2H_2O$	$RuC_{17}H_{24}N_7O_{4.50}$	$RuC_{27}H_{25}Cl_2N_{11}O_8$
M	418.46	499.50	803.55
Radiation	Mo Kα	Mo Kα	Mo Kα
T (K)	298(2)	293(2)	293(2)
Crystal symmetry	monoclinic	monoclinic	monoclinic
Space group	$P2_1/n$	$C2/c$	$P2_1/n$
a (Å)	8.791(1)	18.624(6)	14.6380(13)
b (Å)	16.992(2)	17.083(6)	15.5770(14)
c (Å)	13.516(1)	15.571(5)	14.8802(13)
β (°)	91.201(9)	123.557(4)	108.968(2)
V (Å^3)	2018.5(4)	4128(2)	3208.7(5)
Z	4	8	4
μ (mm^{-1})	0.102	0.801	0.723
D_{calc} (g cm^{-3})	1.377	1.607	1.663
R_1	0.062	0.0275	0.0680
wR_2	0.118	0.0678	0.1446
Goodness-of-fit	0.912	1.099	1.039

Table 2
Selected bond distances (Å) and bond angles (°) and their standard deviation for L, $[Ru^{II}(acac)_2L]\cdot 0.5H_2O$ (**1**) and $[Ru^{II}(bpy)_2L](ClO_4)_2$ (**2**)

L		**1**		**2**	
Bond distances (Å)					
N(1a)–N(2a)	1.384(4)	Ru–N(1)	2.040(2)	Ru(1)–N(1)	2.077(6)
N(2a)–C(6a)	1.398(5)	Ru–N(4)	1.913(2)	Ru(1)–N(4)	1.996(5)
N(3a)–C(6a)	1.336(5)	Ru–O(1)	2.0346(19)	Ru(1)–N(8)	2.060(6)
N(3a)–N(4a)	1.311(5)	Ru–O(2)	2.0419(18)	Ru(1)–N(9)	2.048(6)
N(4a)–C(7a)	1.348(5)	Ru–O(3)	2.048(2)	Ru(1)–N(10)	2.074(5)
N(6a)–C(7a)	1.342(6)	Ru–O(4)	2.0312(19)	Ru(1)–N(11)	2.055(6)
N(5a)–N(6a)	1.336(5)	N(3)–N(4)	1.345(3)	N(3)–N(4)	1.334(7)
N(5a)–C(6a)	1.319(5)	N(5)–N(6)	1.357(3)	N(5)–N(6)	1.302(8)
Bond angles (°)					
C(2a)–N(1a)–N(2a)	104.5(4)	N(4)–Ru–N(1)	80.11(9)	N(4)–Ru(1)–N(11)	97.8(2)
C(4a)–N(2a)–N(1a)	111.3(4)	N(4)–Ru–O(4)	89.95(8)	N(9)–Ru(1)–N(11)	94.9(2)
C(4a)–N(2a)–C(6a)	131.0(4)	N(1)–Ru–O(4)	92.42(9)	N(4)–Ru(1)–N(8)	87.1(2)
N(1a)–N(2a)–C(6a)	117.7(4)	N(4)–Ru–O(3)	178.61(8)	N(9)–Ru(1)–N(8)	79.3(2)
N(4a)–N(3a)–C(6a)	117.5(4)	N(1)–Ru–O(3)	98.79(8)	N(11)–Ru(1)–N(8)	172.7(2)
N(3a)–N(4a)–C(7a)	116.9(4)	O(4)–Ru–O(3)	90.95(8)	N(4)–Ru(1)–N(10)	173.3(2)
C(6a)–N(5a)–N(6a)	116.8(4)	N(4)–Ru–O(2)	95.82(8)	N(9)–Ru(1)–N(10)	91.8(2)
N(5a)–N(6a)–C(7a)	117.0(4)	O(4)–Ru–O(2)	86.24(8)	N(11)–Ru(1)–N(10)	78.2(2)
N(1a)–C(2a)–C(3a)	111.3(4)	O(3)–Ru–O(2)	85.29(8)	N(8)–Ru(1)–N(10)	97.4(2)
N(1a)–C(2a)–C(1a)	120.3(5)	N(4)–Ru–O(1)	92.40(8)	N(4)–Ru(1)–N(1)	78.4(2)
C(3a)–C(2a)–C(1a)	128.4(5)	N(1)–Ru–O(1)	88.30(8)	N(9)–Ru(1)–N(1)	170.7(2)
C(4a)–C(3a)–C(2a)	107.3(5)	N(1)–Ru–O(2)	175.73(8)	N(11)–Ru(1)–N(1)	91.4(2)
C(3a)–C(4a)–N(2a)	105.6(4)	O(4)–Ru–O(1)	177.62(7)	N(8)–Ru(1)–N(1)	94.9(2)
C(3a)–C(4a)–C(5a)	129.6(5)	O(3)–Ru–O(1)	86.70(8)	N(10)–Ru(1)–N(1)	96.2(2)
N(2a)–C(4a)–C(5a)	124.9(4)	O(2)–Ru–O(1)	93.19(8)	N(4)–Ru(1)–N(9)	93.9(2)

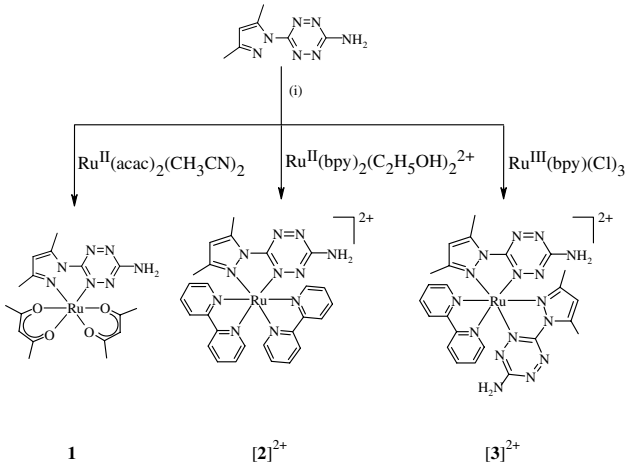

Scheme 2. (i) EtOH, Δ.

$[(bpy)_2Ru^{II}(\mu\text{-bpytz})Ru^{II}(bpy)_2]^{4+}$ at 2.114(16) Å [2b]. The Ru^{II}–N(tetrazine) distances found in dinuclear complexes such as $[(bpy)_2Ru^{II}(\mu\text{-bpytz})Ru^{II}(bpy)_2]^{4+}$ [2b] and $[(acac)_2Ru^{II}(\mu\text{-bptz})Ru^{II}(acac)_2]$ [2d] are 1.976(14)/1.993(11) and 1.946(6)/1.943(6) Å, respectively, which is appreciably longer than the 1.912(3) Å observed for **1**.

The RuN_6 center in **2** is more distorted octahedral. The distortion of the coordination sphere is primarily caused by the small bite angles, viz., 79.3(2)° (bpy), 78.2(2)° (bpy) and 78.5(2)° (L). The average *trans* angle is 172.23(2)°. The Ru^{II}–N(bpy) distances lie between 2.048(6) and 2.074(5) Å which is comparable with reported data of similar species [13]. The Ru^{II}–N(1)(pyrazolyl) and Ru^{II}–N(4)(tetrazine) distances are at 2.077(6) and 1.996(5) Å, respectively. Thus, the back bonding

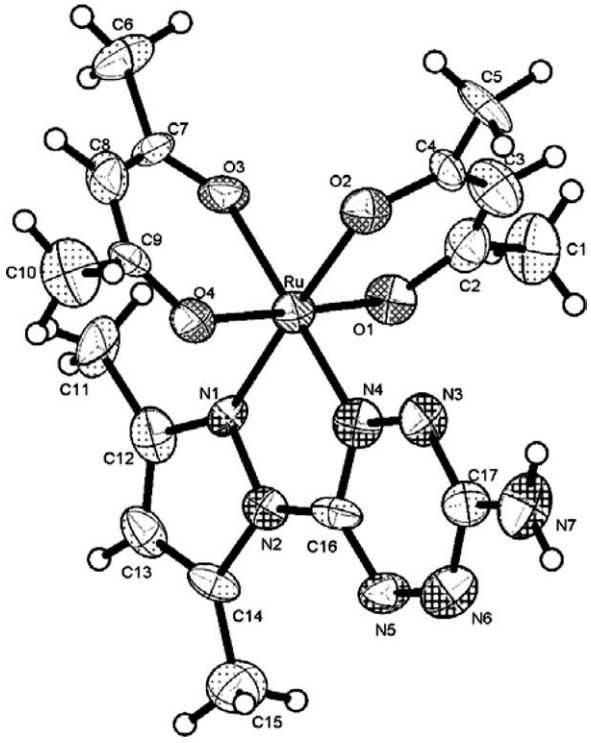

Fig. 2. ORTEP diagram of the complex $[Ru^{II}(acac)_2L]\cdot 0.5H_2O$ (**1**). Ellipsoids are drawn at 50% probability. Water of crystallization has been removed for clarity.

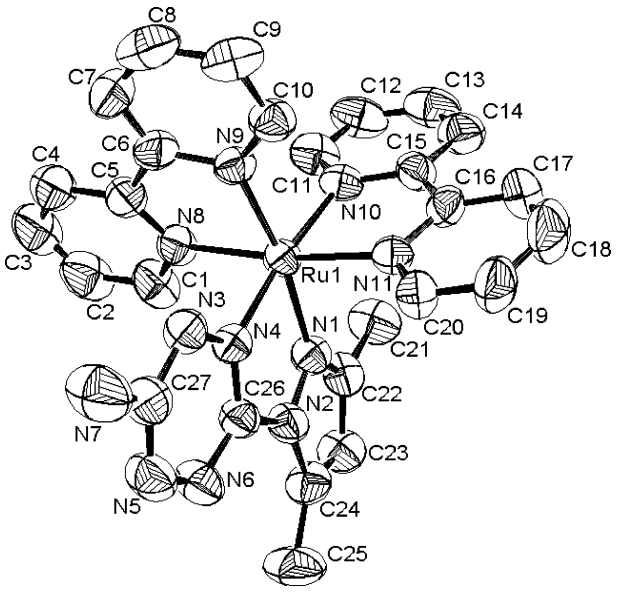

Fig. 3. ORTEP diagram of the complex cation $[Ru^{II}(bpy)_2L]^{2+}$ of (**2**). Ellipsoids are drawn at 50% probability.

effect $d\pi(Ru^{II}) \rightarrow \pi^*$(tetrazine) is also reflected in the structure of **2**. The presence of π-acidic bpy ancillary ligands competing with L in **2** is held responsible for the observed Ru–N bond lengthening, leading to appreciable decreasing $Ru^{II} \rightarrow \pi^*$ back donation on moving from **1** to **2**.

The strong $Ru^{II} \rightarrow \pi^*$(tetrazine) back bonding in **1** is also reflected in the appreciable lengthening of the tetrazine bond lengths involving the coordinated nitrogen donor center [N(4)], C(16)–N(4) 1.377(7) and N(3)–N(4) 1.345(3) Å, as compared to those of the free ligand (L), C(6)–N(3), 1.336(5) and N(3)–N(4), 1.311(5) Å. However, in the case of the corresponding bipyridine complex (**2**) only a slight increase in bond distances has been observed [C(26)–N(4), 1.340(8) and N(3)–N(4), 1.334(7) Å], which is certainly due to the existence of much weaker $Ru^{II} \rightarrow \pi^*$(tetrazine) back bonding in **2** compared to **1** as stated above.

3.3. ^1H NMR spectra

^1H NMR spectra of the complexes **1**, **2** and **3** were recorded in $CDCl_3$ (**1**) and $(CD_3)_2SO$. The spectra are shown in Fig. 4. The unsymmetrical nature of L makes the protons associated with the chelate rings magnetically different. Therefore, the ^1H NMR spectrum of **1** displays three distinct singlets corresponding to two acac CH protons (δ, 5.57 and 5.20 ppm) and one CH proton associated with L (δ, 5.92 ppm) (Fig. 4(a)). The NH_2 protons of L appear as a slightly broad singlet at 4.92 ppm. In addition, six singlets are observable in the upfield region at 2.85, 2.24, 2.18, 2.16, 2.11 and 1.92 ppm, corresponding to four and two CH_3 groups associated with acac and L, respectively.

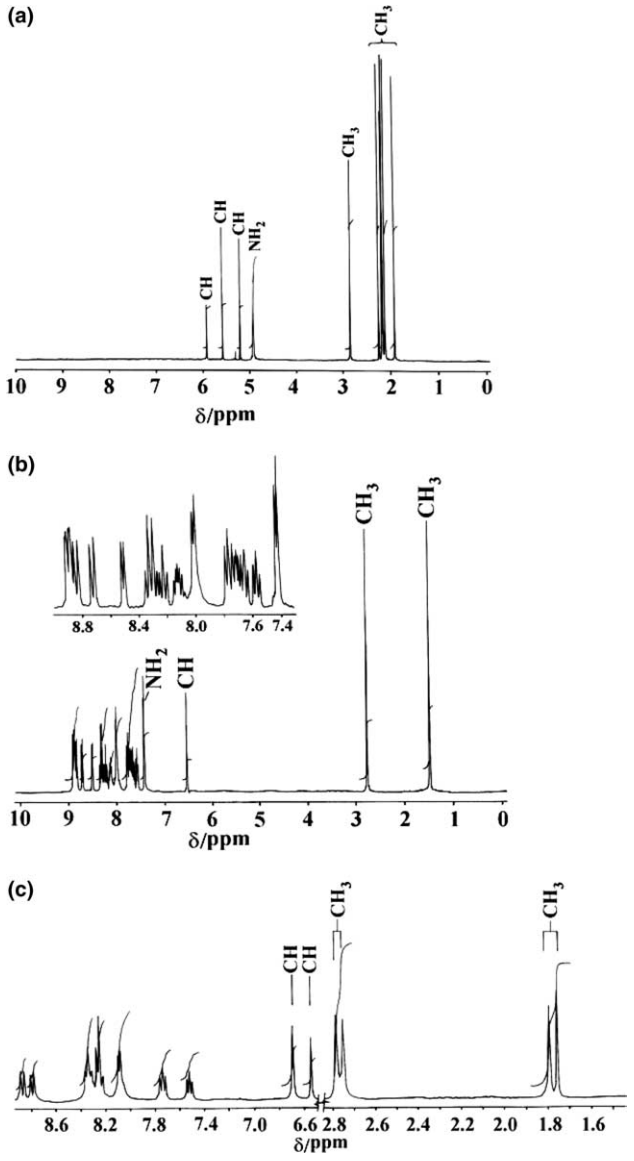

Fig. 4. ^1H NMR spectra of (a) $[Ru^{II}(acac)_2L]$ (**1**) in $CDCl_3$, (b) $[Ru^{II}(bpy)_2L](ClO_4)_2$ (**2**) in $(CD_3)_2SO$, inset shows the expanded aromatic region (δ, 7.4–9.0 ppm), (c) $[Ru^{II}(bpy)(L)_2](ClO_4)_2$ (**3**) in $(CD_3)_2SO$ (solvent peaks are substracted for clarity).

Similarly, the four pyridine rings of two bpy ligands in **2** are inequivalent. Complex **2** should thus exhibit 16 non-equivalent "aromatic" proton signals. Since the electronic environment of many such hydrogen atoms is similar, their signals may appear in a narrow chemical shift range. In fact, the "aromatic region" of the spectrum of **2** is complicated due to the overlapping of several signals, which has essentially precluded the identification of individual resonances (Fig. 4(b)). However, a direct comparison of the intensity of these signals with that of the clearly observable CH (6.53 ppm) and CH_3 (2.76 and 1.47 ppm) protons of coordinated L in the upfield region revealed the presence of the expected 16 aromatic protons. The NH_2 protons of L appear at 7.4 ppm.

In **3** two distinct CH signals at 6.69 and 6.54 ppm and four CH_3 signals at 2.77, 2.74, 1.79 and 1.47 ppm, corresponding to two L, were observed (Fig. 4(c)). The eight protons of bpy and the NH_2 protons of L appear between 7.4 and 9.0 ppm as partially overlapping signals.

3.4. Metal oxidation

Compounds **1**–**3** exhibit one quasi-reversible Ru^{III}/Ru^{II} couple each at $E_{1/2}$ = 0.28, 1.34 and 1.50 V versus SCE, respectively (Table 3, Fig. 5). The data reveal that a redox potential shift of >1.0 V has taken place on switching from the acac ancillary ligands in $[Ru(acac)_2(L)]$ (**1**) to the bpy co-ligands in $[Ru(bpy)_2(\mathbf{L})](ClO_4)_2$ (**2**). The presence of electron-rich acac ligands in **1** clearly stabilizes the Ru^{III} state [14].

The combination of two bpy ligands and one L ligand around the Ru^{II} center in **2** shifted the Ru^{III}/Ru^{II} couple to 1.34 V which is even higher than that of $[Ru^{II}(bpy)_3]^{2+}$ ($E_{1/2}$ = 1.29 V versus SCE) [15]. This implies that the donor strength of L is lower than that of bpy. It may be noted that the first Ru^{III}/Ru^{II} couple of the related diruthenium complex $[(bpy)_2Ru(\mu\text{-bpytz})Ru(bpy)_2]^{4+}$ appears at 1.25 V [2b].

On the other hand, the replacement of two bpy ligands from $[Ru^{II}(bpy)_3]^{2+}$ by two ligands L in **3** increases the $Ru^{II} \rightarrow Ru^{III}$ oxidation potential further to 1.50 V. Thus, successive exchange of bpy by L from $Ru(bpy)_3^{2+}$ via $Ru(bpy)_2(L)^{2+}$ to $Ru(bpy)(L)_2^{2+}$ enhances the stability of the Ru^{II} state.

3.5. Ligand reduction

Complex **1** shows one reversible reduction at −1.33 V versus SCE. Since tetrazines are known to undergo facile reduction at relatively low potentials due to the low lying π* orbital [1–3], the observed reduction is therefore considered to involve the tetrazine function of coordinated L.

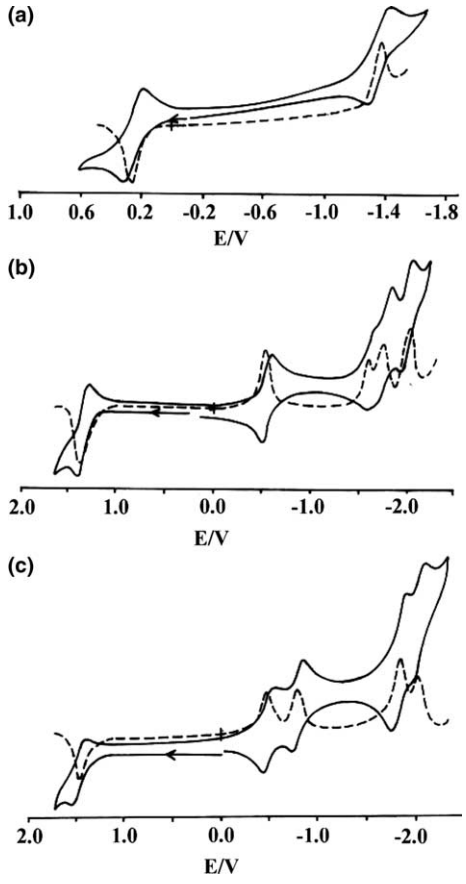

Fig. 5. Cyclic (—) and differential pulse (------) voltammograms of (a) $[Ru^{II}(acac)_2L]$ (**1**) in CH_2Cl_2, (b) $[Ru^{II}(bpy)_2L](ClO_4)_2$ (**2**) and (c) $[Ru^{II}(bpy)(L)_2](ClO_4)_2$ (**3**) in CH_3CN at 298 K.

Table 3
Electrochemical,[a] electronic spectra[a] and spectroelectrochemical correlation data[b]

Compound	Ru^{III}–Ru^{II} couple, E^0_{298}/V (ΔE_p, mV)	Ligand reductions, E^0_{298}/V (ΔE_p, mV)		$\Delta E_{1/2}$[c] (V)	UV–Vis, λ/nm (ε/M^{-1} cm^{-1})	ν(MLCT) (cm^{-1})	
		L-based	bpy-Based			Observed	Calculated[d]
1	0.28(110)	−1.33(110)		1.61	600 (13 650), 366 (9700), 268 (71 250), 218 (30 100)	16 666	15 984
2	1.34(80)	−0.55(100)		1.89	538 (8000), 400 (4800),	18 587	18 242
			−1.55(60)	2.89	278 (52 400), 214 (23 000)	25 000	26 307
			−1.75(100)				
			−1.98(60)				
3	1.50(70)	−0.47(100)		1.97	540 (10 380), 480 (7230),	18 518	18 888
		−0.78(100)		2.28	276 (47 260), 206 (56 400)	20 833	21 388
			−1.80(60)				
			−2.02(60)				

[a] **1** in CH_2Cl_2 and **2**/**3** in CH_3CN.
[b] As stated in the text.
[c] Calculated by Eq. (2) in the text.
[d] Calculated by Eq. (1) in the text.

Similarly, the reduction of the tetrazine in **2** appears at −0.55 V. This substantial increase in the reduction potential by 0.78 V on moving from strongly σ-donating acac as a co-ligand in **1** to π-acidic bpy in **2** parallels to some extent the stabilization of the Ru^{II} state in **2** as compared to **1**.

In addition to the tetrazine-based reduction of L, **2** also shows three more bpy-based quasi-reversible one-electron reduction processes in the range from −1.55 to −1.98 V. Each bpy can accommodate two electrons, therefore, a total of four such reduction waves is expected. Three such waves are detected within the experimental potential limit (−2.0 V versus SCE). The potentials at which the bpy reductions of **2** are observed is consistent with the reduction range of $Ru(bpy)_3^{2+}$ (−1.3 to −1.8 V versus SCE) [16].

Compound **3** contains two tetrazine units from two L ligands, therefore the expected two tetrazine-based one-electron reduction waves were observed at −0.47 and −0.78 V. Two bpy-based reductions appear at −1.80 and −2.02 V. The first tetrazine reduction potential in **3** is slightly less negative relative to **2**, which correlates with the enhanced stabilization of the Ru^{II} state in **3**.

3.6. Spectral properties

Electronic absorption spectra of **1**, **2** and **3** were recorded in CH_2Cl_2 (**1**) and CH_3CN. The spectral data are given in Table 3 and the spectra are shown in Fig. 6. The complexes exhibit strong ligand-based π − π* transitions in the UV region. In the visible region, **1** and **2** display two well separated broad bands at 600/366 and 538/400 nm, respectively, whereas **3** exhibits one main transition at 540 nm with a high-energy shoulder at 480 nm. The lowest energy bands for all the three complexes are attributed to MLCT transitions $d\pi(Ru^{II}) \rightarrow \pi_1^*L$ (where π_1^*L is essentially dominated by the tetrazine moiety) [2]. The higher energy transitions are assigned as $d\pi(Ru^{II}) \rightarrow \pi^*$ (acac), $d\pi(Ru^{II}) \rightarrow \pi^*$(bpy) and $d\pi(Ru^{II}) \rightarrow \pi^*$ L for **1**, **2** and **3**, respectively. This is based on the observation that the reduction of L takes place at a much lower potential than that of bpy. The above assignments find justification through the spectro-electrochemical correlations stated below.

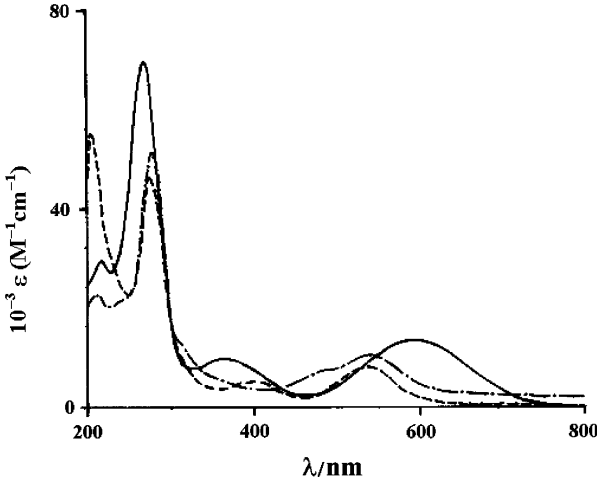

Fig. 6. Electronic spectra of (a) $[Ru^{II}(acac)_2L]$ (**1**) (——), (b) $[Ru^{II}(bpy)_2L](ClO_4)_2$ (**2**) (------) and (c) $[Ru^{II}(bpy)(L)_2](ClO_4)_2$ (**3**) (-·-·-·) in CH_3CN.

3.7. Spectro-electrochemical correlation

The energies of the MLCT transitions at the band maximum can be reproduced with the help of empirical Eqs. (1) and (2) [17]:

$$\nu(\text{MLCT}) = 8065(\Delta E_{1/2}) + 3000\ \text{cm}^{-1}, \quad (1)$$

$$\Delta E_{1/2} = E_{1/2}(Ru^{III}/Ru^{II}) - E_{1/2}(L). \quad (2)$$

Here $E_{1/2}(Ru^{III}/Ru^{II})$ is the potential of the reversible Ru^{III}/Ru^{II} couple, $E_{1/2}(L)$ is that of the first ligand-based reduction and ν(MLCT) is the wave number of the charge transfer band in cm^{-1}. The factor 8065 is used to convert the potential difference ΔE from V into cm^{-1} and the term 3000 cm^{-1} is of empirical origin (reorganization energy of polypyridine ruthenium MLCT transitions). The calculated and experimentally observed MLCT energies are given in Table 3. Using Eqs. (1) and (2) and $\Delta E_{1/2}$ values of 1.61, 1.89/2.89 and 1.97/2.28, for **1**, **2** and **3**, respectively, the calculated ν(MLCT) values agree rather well with the experimental values (Table 3).

3.8. EPR spectra

The in situ generated species $\mathbf{1}^+$ in CH_2Cl_2 at 110 K exhibits a rhombic EPR signal ($g_1 = 2.260$, $g_2 = 2.170$, $g_3 = 1.880$, Fig. 7(a)), typical of low-spin Ru^{III}. The g anisotropy $g_1 - g_3 = 0.380$ and the average g factor of $\langle g \rangle = 2.11$), derived from $\langle g \rangle = [1/3(g_1^2 + g_2^2 + g_3^2)]^{1/2}$ indicate a slightly distorted octahedral arrangement around the ruthenium center [18] as consistent with the molecular structure of **1**. The electrochemically generated $\mathbf{2}^+$ in CH_3CN failed to show any EPR signals at 110 K, however, at 4 K it displays a poorly resolved rhombic type EPR signal with $g_1 = 2.50$, $g_2 = 2.360$ and an undetectable g_3 component (probably < 1.8). On the other hand, the in situ generated $\mathbf{3}^+$ did not show any EPR response even at 4 K, which signifies rapid relaxation due to excited paramagnetic states lying close to the doublet ground state.

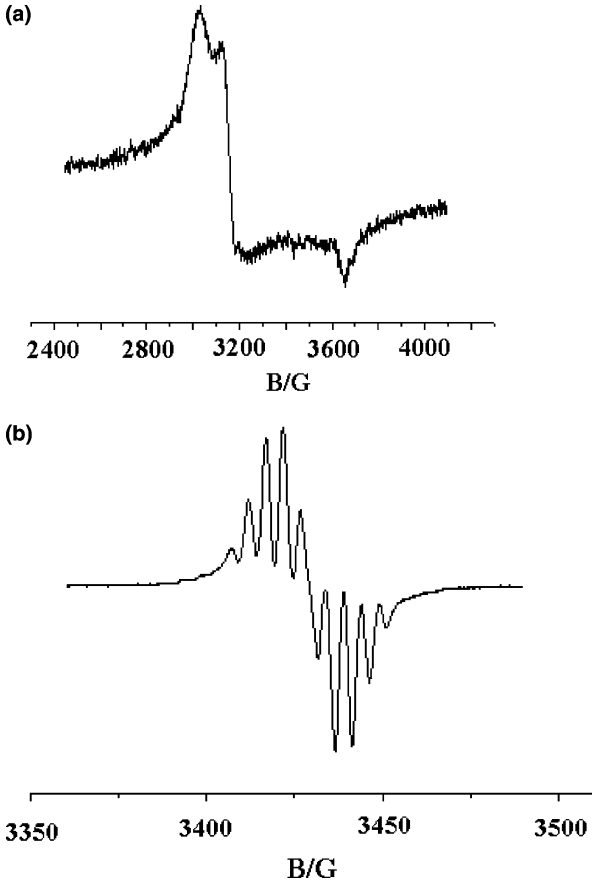

Fig. 7. EPR spectra of (a) $\mathbf{1}^{+}$ in CH_2Cl_2 at 100 K and (b) $\mathbf{1}^{-}$ in CH_2Cl_2 at 300 K.

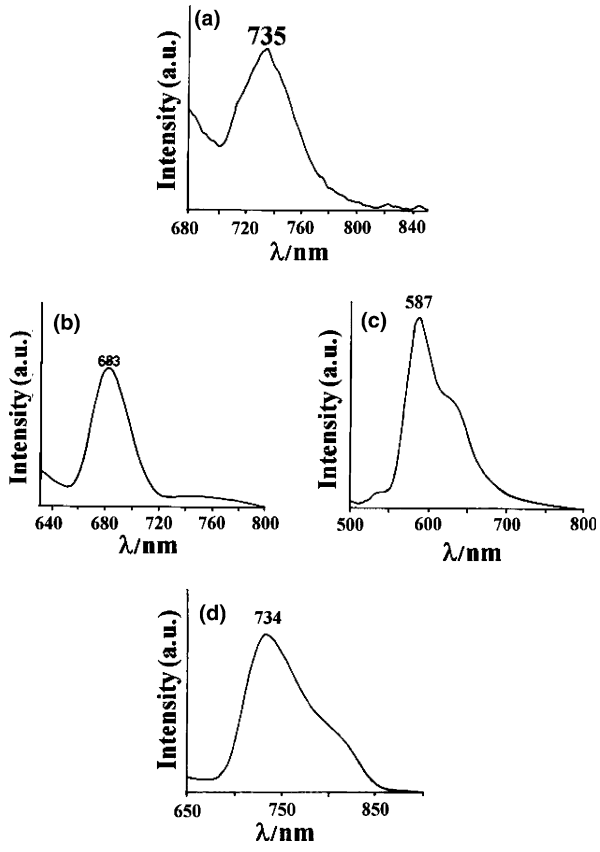

Fig. 8. Emission spectra of (a) **1** ($\lambda_{excitation}$, 592 nm), (b) **2** ($\lambda_{excitation}$, 530 nm), (c) **2** ($\lambda_{excitation}$, 413 nm) and (d) **3** ($\lambda_{excitation}$, 524 nm) in ethanol–methanol (4:1) glass at 77 K.

In situ generated reduced species $\mathbf{1}^{-}$ (in CH_2Cl_2), $\mathbf{2}^{-}$ and $\mathbf{3}^{-}$ (in CH_3CN) exhibit multiple line EPR spectra at 300 K due to hyperfine coupling from four different ^{14}N atoms of the tetrazine ring of L, the signals are centered at $g = 1.9962$, 1.9991 and 1.9984, respectively (Fig. 7(b)) [2,19].

3.9. Emission spectra

Emission properties of the complexes were studied in EtOH–MeOH (4:1) at 77 K. The spectra are shown in Fig. 8. Excitations of the complexes **1**, **2** and **3** at 592, 530/413 and 534 nm, respectively, result in emissions with maxima at 735 nm (quantum yield, $\Phi = 0.65 \times 10^{-2}$), 682/586 nm (quantum yield, $\Phi = 1.8 \times 10^{-1}$, 1.1×10^{-1}) and 734 nm (quantum yield, $\Phi = 1.15 \times 10^{-2}$), respectively, with vibrational structures characteristic of emissions from a ^{3}MLCT excited state [20]. The origin of the emissions was further confirmed by the excitation spectra of the same solutions in each case. The observed moderately strong emissions for **1** and **3** presumably involve primarily L. On the other hand, **2** appears to exhibit strong emissions from both the bpy and L-based MLCT transitions.

4. Conclusion

Although tetrazine based ligands are quite popular in developing polynuclear complexes for varying perspectives, rather rare mononuclear complexes **1**, **2** and **3** have been synthesized using hitherto unexplored tetrazine derived ligand, 3-amino-6-(3,5-dimethylpyrazol-1-yl)-1,2,4,5-tetrazine (L) in combination with σ-donating acetylacetonate and π-accepting bipyridine co-ligands. Structural studies reveal that the presence of electron-rich acetylacetonate co-ligands attributes to a strong $Ru^{II} \rightarrow \pi^*$ (tetrazine) back bonding in **1** which is much stronger than that in the corresponding mononuclear bipyridine derivative (**2**) as well as that in the analogous dinuclear complexes $[(bpy)_2Ru^{II}(\mu\text{-bpytz})Ru^{II}(bpy)_2]^{4+}$ and $[(acac)_2Ru^{II}(\mu\text{-bptz})Ru^{II}(acac)_2]$.

Acknowledgements

Financial support received from the Council of Scientific and Industrial Research, New Delhi (India), the DAAD, the DFG and the FCI (Germany) is gratefully acknowledged. We are grateful to Professor Seik

Weng Ng, Institute of Postgraduate Studies, University of Malaya, Kuala Lumpur, Malaysia for solving the crystal structure of L. Special acknowledgement is made to the Sophisticated Analytical Instrument Facility, Indian Institute of Technology, Bombay, for providing the NMR facility. X-ray structural studies of L were carried out at the National Single Crystal Diffractometer Facility, Indian Institute of Technology, Bombay.

Appendix A. Supplementary data

Crystallographic data for the structural analysis have been deposited with the Cambridge Structural Database, CCDC Nos. 242646, 242644 and 242645, for compounds L, **1** and **2**, respectively. Supplementary data are available from CCDC, 12 Union Road Cambridge CB2 1EZ, UK

Electrospray mass
spectral data of **1** (Fig. S1a), **2** (Fig. S1b) and **3** (Fig. S1c). Supplementary data associated with this article can be found, in the online version

References

[1] W. Kaim, Coord. Chem. Rev. 230 (2002) 127.
[2] (a) B. Sarkar, W. Kaim, A. Klein, B. Schwederski, J. Fiedler, C. Duboc-Toia, G.K. Lahiri, Inorg. Chem. 42 (2003) 6172;
(b) B. Sarkar, R.H. Laye, B. Mondal, S. Chakraborty, R.L. Paul, J.C. Jeffery, V.G. Puranik, M.D. Ward, G.K. Lahiri, J. Chem. Soc., Dalton Trans. (2002) 2097;
(c) A. Singh, N. Singh, D.S. Pandey, J. Organomet. Chem. 642 (2002) 48;
(d) S. Chellamma, M. Lieberman, Inorg. Chem. 40 (2001) 3177;
(e) M. Glockle, W. Kaim, J. Fiedler, Z. Anorg. Allg. Chem. 627 (2001) 1141;
(f) S. Roche, L.J. Yellowlees, J.A. Thomas, Chem. Commun. (1998) 1429;
(g) V. Kasack, W. Kaim, H. Binder, J. Jordanov, E. Roth, Inorg. Chem. 34 (1995) 1924;
(h) J. Poppe, M. Moscherosch, W. Kaim, Inorg. Chem. 32 (1993) 2640;
(i) W. Kaim, V. Kasack, Inorg. Chem. 29 (1990) 4696;
(j) M.H. Zaghal, H.A. Qaseer, Inorg. Chim. Acta 163 (1989) 193;
(k) S. Ernst, V. Kasack, W. Kaim, Inorg. Chem. 27 (1988) 1146.
[3] (a) D. Brown, S. Muranjan, Y. Jang, R. Thummel, Org. Lett. 4 (2002) 1253;
(b) M. Chandra, A.N. Sahay, D.S. Pandey, M.C. Puerta, P. Valerga, J. Organomet. Chem. 648 (2002) 39;
(c) J. Poppe, W. Kaim, A. Ben Altabef, N.E. Katz, J. Chem. Soc., Perkin Trans. (1993) 2105 (1972–1999);
(d) J.E.B. Johnson, C. De Groff, R.R. Ruminski, Inorg. Chim. Acta 187 (1991) 73;
(e) T.S. Akasheh, D. Marji, Z.M. Al-Ahmed, Inorg. Chim. Acta 141 (1988) 125;
(f) T.S. Akasheh, Z.M. El-Ahmed, Chem. Phys. Lett. 152 (1988) 414.
[4] C. Glidewell, P. Lightfoot, B.J.L. Royles, D.M. Smith, J. Chem. Soc., Perkin Trans. (1997) 1167.
[5] T. Kobayashi, Y. Nishina, K. Shimizu, G.P. Satô, Chem. Lett. (1988) 1137.
[6] B.P. Sullivan, D.J. Salmon, T.J. Meyer, Inorg. Chem. 17 (1978) 3334.
[7] S. Anderson, K.R. Seddon, J. Chem. Res. (S) (1979) 74.
[8] D.T. Sawyer, A. Sobkowiak, J.L. Roberts Jr., Electrochemistry for Chemists, Wiley, New York, 1995.
[9] W. Kaim, S. Ernst, V. Kasack, J. Am. Chem. Soc. 112 (1990) 173.
[10] (a) E.F. Godefroi, E.L. Little, J. Org. Chem. 21 (1956) 1163;
(b) P. Chen, R. Duesing, D.K. Graff, T.J. Meyer, J. Phys. Chem. 95 (1991) 5850.
[11] G.M. Sheldrick, SHELX-97 Program for Crystal Structure Solution and Refinement, University of Göttingen, Göttingen, Germany, 1997.
[12] N. Chanda, B. Mondal, V.G. Puranik, G.K. Lahiri, Polyhedron 21 (2002) 2033.
[13] (a) S. Chakravorty, R.H. Laye, P. Munshi, R.L. Paul, M.D. Ward, G.K. Lahiri, J. Chem. Soc., Dalton Trans. (2002) 2348;
(b) S. Chakraborty, R.H. Laye, R.L. Paul, R.G. Gonnade, V.G. Puranik, M.D. Ward, G.K. Lahiri, J. Chem. Soc., Dalton Trans. (2002) 1172;
(c) S. Chakraborty, M.G. Walawalkar, G.K. Lahiri., J. Chem. Soc., Dalton Trans. (2000) 2875.
[14] (a) S. Patra, B. Sarkar, S.M. Mobin, W. Kaim, G.K. Lahiri, Inorg. Chem. 42 (2003) 6469;
(b) S. Patra, T.A. Miller, B. Sarkar, M. Niemeyer, M.D. Ward, G.K. Lahiri, Inorg. Chem. 42 (2003) 4707;
(c) S. Patra, B. Mondal, B. Sarkar, M. Niemeyer, G.K. Lahiri, Inorg. Chem. 42 (2003) 1322.
[15] (a) A. Ceulemansm, L.G. Vanquickenborne, J. Am. Chem. Soc. 103 (1981) 2238;
(b) M.J. Root, E. Deutsch, Inorg. Chem. 24 (1985) 1464;
(c) R. Alsfasser, R.V. Eldik, Inorg. Chem. 35 (1996) 628;
(d) B.J. Coe, T.J. Meyer, P.C. White, Inorg. Chem. 34 (1995) 593.
[16] (a) S. Bhattacharya, Polyhedron 12 (1993) 235;
(b) C.M. Elliott, J. Chem. Soc., Chem. Commun. (1980) 261;
(c) N.E. Tokel-Takvoryan, J. Am. Chem. Soc. 95 (1973) 6583;
(d) D.E. Morris, K.W. Hanck, M.K. DeArmond, Inorg. Chem. 24 (1985) 977.
[17] (a) B.K. Ghosh, A. Chakravorty, Coord. Chem. Rev. 95 (1989) 239;
(b) B.K. Santra, G.K. Lahiri, J. Chem. Soc., Dalton Trans. (1997) 129;
(c) E.S. Dosworth, A.B.P. Lever, Chem. Phys. Lett. 124 (1986) 152.
[18] (a) S. Patra, B. Sarkar, S. Ghumaan, J. Fiedler, W. Kaim, G.K. Lahiri, J. Chem. Soc., Dalton Trans. (2004) 754;
(b) N. Chanda, B. Sarkar, J. Fiedler, W. Kaim, G.K. Lahiri, J. Chem. Soc., Dalton Trans. (2003) 3550;
(c) S. Kar, T.A. Miller, B. Sarkar, B. Pradhan, T. Kundu, M.D. Ward, G.K. Lahiri, J. Chem. Soc., Dalton Trans. (2003) 2591;
(d) B.K. Santra, M. Menon, C.K. Pal, G.K. Lahiri, J. Chem. Soc., Dalton Trans. (1997) 1387.
[19] (a) W. Kaim, S. Kohlmann, Inorg. Chem. 25 (1986) 3442;
(b) W. Kaim, S. Ernst, S. Kohlmann, P. Welkering, Chem. Phys. Lett. 118 (1985) 431.
[20] A. Juris, V. Balzani, F Barigelletti, S. Campagna, P. Belser, A. von Zelewski, Coord. Chem. Rev. 84 (1988) 85.